Treatment of locking behaviour for displacement-based finite element analysis of composite beams

R. Emre Erkmen[*1], Mark A. Bradford[2a] and Keith Crews[1b]

[1]*School of Civil and Environmental Engineering, University of Technology, Sydney, NSW 2007, Australia*
[2]*School of Civil and Environmental Engineering, The University of New South Wales,
Sydney, NSW 2052, Australia*

Abstract.   In the displacement based finite element analysis of composite beams that consist of two Euler-Bernoulli beams juxtaposed with a deformable shear connection, the coupling of the displacement fields may cause oscillations in the interlayer slip field and reduction in optimal convergence rate, known as slip-locking. In this study, the B-bar procedure is proposed to alleviate the locking effects. It is also shown that by changing the primary dependent variables in the mathematical model, to be able to interpolate the interlayer slip field directly, oscillations in the slip field can be completely eliminated. Examples are presented to illustrate the performance and the numerical characteristics of the proposed methods.

Keywords: composite beam; slip-locking; B-bar formulation; change of primary variables

1. Introduction

Composite beams that consist of two or more components juxtaposed with a shear connection are widely used in the design of bridges and buildings. The interlayer slip between the two components affects the behaviour of the beam significantly, especially the serviceability limit state response. The deflections depend primarily on the stiffness of the shear connectors and it cannot be determined accurately unless the interlayer slip between the two components is considered. The mathematical model for composite beams with flexible shear connectors was initially introduced in the seminal paper of Newmark *et al.* (1951), in which two Euler-Bernoulli beams are connected by assuming that vertical separation does not occur between the components. Subsequently, several displacement-based finite element formulations were developed based on Newmark's model, which include the works of Arizumi *et al.* (1981), Daniels and Crisinel (1993), Ranzi *et al.* (2004), Ranzi and Bradford (2009), Dall'Asta and Zona (2002). However, for stiff interlayer connections, displacement-based finite element formulations may suffer from the so-called slip-locking phenomenon because of the coupling between the displacement fields. In order to overcome the limitations of displacement-based finite element formulations, mixed and force-

---

∗Corresponding author, Lecturer, E-mail: emre.erkmen@uts.edu.au
[a]Scientia Professor
[b]Professor

based finite element formulations were developed by Salari *et al.* (1998), Ayoub and Filippou (2000), Ayoub (2005), Dall'Asta and Zona (2004a). The consistent interpolation strategy was used by Dall'Asta and Zona (2004b) to develop a locking-free displacement-based finite element formulation in which additional internal nodes were introduced. Erkmen and Bradford (2011a) used the kinematic interpolation strategy and assumed strain-mixed formulations to alleviate locking behaviour for stiff connections. Finite element formulations based on the exact solution of the homogenous form of the equilibrium equations can be found in Faella *et al.* (2002) and Ranzi *et al.* (2004). A proof of the "exactness" of nodal values for general non-homogenous loading cases is presented in Erkmen and Bradford (2011a). Similarities in the locking mechanisms in Timoshenko beams and composite beams analysed using Newmark's model are also discussed in Erkmen and Bradford (2011a), while a mesh-free approach that eliminates slip-locking was recently developed by Erkmen and Bradford (2010b). A shear-deformable two-layer beam model with independent shear strains in both layers is analytically solved and a corresponding FE with "exact" stiffness matrix is developed in Nguyen *et al.* (2011a), where shear connection is modelled through a continuous relationship. An "exact" finite element solution for shear-deformable two-layer composite beams with discontinuous shear connections is presented in Nguyen et al (2011b). A comparison between the two-layer composite beam models and a study of the hierarchy between these models can be found in Martinelli *et al.* (2012).

The objective of this paper is to introduce efficient and simple displacement-based finite element formulations to alleviate the locking effects in the finite element analysis of composite beams. A finite element method based on the primary variable fields of Newmark's formulation is proposed by using the B-bar procedure which was originally developed by Hughes and Tezduyar (1981) in order to eliminate shear locking in the finite element analysis of Mindlin plates. It is also shown that by changing the primary variable fields of Newmark's mathematical model, slip-locking can be completely eliminated in the analysis of composite beams. This approach was conveniently used for the nonlinear analysis of composite beams by Pi et al. (2006) and later for curved composite beams by Erkmen and Bradford (2009, 2010a,b, 2011b). Cho and Atluri (2001) used this approach in the context of Timoshenko beams to eliminate shear locking. Numerical examples are presented to illustrate the performance and the numerical characteristics of the proposed methods.

2. Composite beam kinematics

2.1 Displacements and strains

The composite beam-column is composed of a top and a bottom Euler-Bernoulli beam which are referred to as layers 1 and 2. The composite cross-section is thus represented as $A=A_1+A_2$, where A_1 and A_2 are the cross-sections of layers 1 and 2, respectively as shown in Fig. 1(a). According to Newmark's model, the strain diagram is determined uniquely by the curvature of the vertical deflection v'' with respect to an arbitrary reference axis and the derivatives of the longitudinal displacements at the centroid of each layer w_1' and w_2' as shown in Fig. 1. Slip displacement between the two layers Γ can be obtained in terms of the slope of the vertical deflection v' and the longitudinal displacements at the centroids of the layers w_1 and w_2.

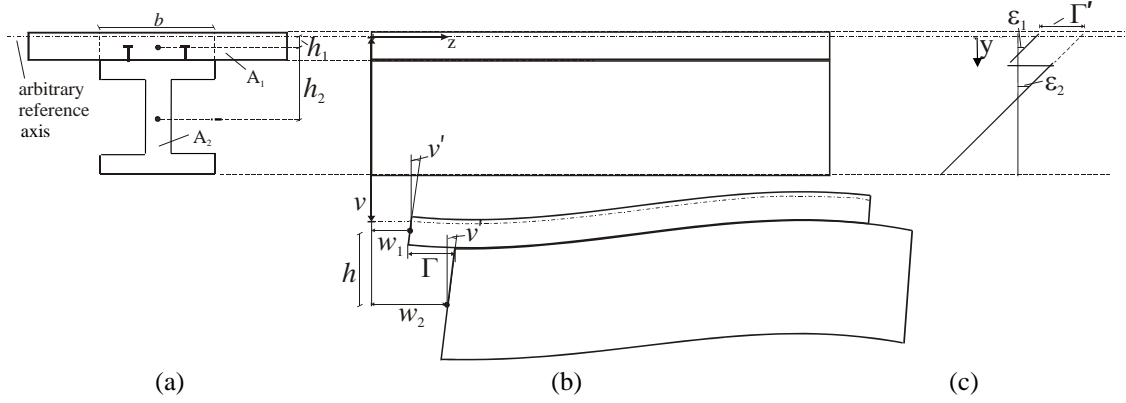$$\varepsilon_1 = w_1' - \left(y - h_1\right)v'' \tag{1}$$

Fig. 1 Composite beam (a) cross-section, (b) displacements, (c) strains

$$\varepsilon_2 = w_2' - (y - h_2)v'' \tag{2}$$

and

$$\Gamma = w_2 - w_1 + hv' \tag{3}$$

where h is the distance between the centroids of the beams, i.e., $h=h_2-h_1$, and prime (') denotes the derivative with respect to longitudinal coordinate z.

3. Finite element formulations

3.1 Basic displacement based finite element formulation

A displacement based finite element formulation can be developed by employing the total potential energy functional Π, i.e.

$$\Pi = \tfrac{1}{2} \int_L \int_{A_1} E_1 \varepsilon_1^2 \mathrm{d}A\mathrm{d}z + \tfrac{1}{2} \int_L \int_{A_2} E_2 \varepsilon_2^2 \mathrm{d}A\mathrm{d}z + \tfrac{1}{2} \int_L \int_b \rho \Gamma^2 \mathrm{d}x\mathrm{d}z - \Pi_{ext} \tag{4}$$

where the first and second integrals are the elastic bending energies of the two Euler-Bernoulli beam components, the third integral is due to the elastic deformations of the shear connection where ρ is its elastic stiffness (force/length^3) defined as the shear stress in longitudinal direction per unit slip, b is the width of the effective interface surface between the two beam components, and Π_{ext} is the work done by the external forces. In a displacement-based finite element formulation, the longitudinal displacement fields w_1 and w_2 and the derivative of the vertical displacement field v' can be expressed using interpolation functions as

$$\begin{Bmatrix} w_1 \\ w_2 \\ v' \end{Bmatrix} = \begin{bmatrix} \mathbf{M}(z) & \mathbf{0} & \mathbf{0} \\ \mathbf{0} & \mathbf{M}(z) & \mathbf{0} \\ \mathbf{0} & \mathbf{0} & \mathbf{N}'(z) \end{bmatrix} \begin{Bmatrix} \mathbf{w}_{N1} \\ \mathbf{w}_{N2} \\ \mathbf{v}_N \end{Bmatrix} = \mathbf{B}_\Gamma(z)\mathbf{U} \tag{5}$$

where $\mathbf{M}(z)$ and $\mathbf{Z}(z)$ are vectors of the interpolation functions for the longitudinal and the vertical displacement fields, respectively. In Eq. (5), $\mathbf{B}_\Gamma(z)$ is the discrete interlayer slip matrix and $\mathbf{U}$ is the vector of nodal displacements composed of the vectors of nodal longitudinal displacements at the centroids of both beams $\mathbf{w}_{N1}$, $\mathbf{w}_{N2}$ and the vertical displacement $\mathbf{v}_M$, i.e.

$$\mathbf{U}^{\mathrm{T}} = \left\langle \mathbf{w}_{N1}^{\mathrm{T}} \quad \mathbf{w}_{N2}^{\mathrm{T}} \quad \mathbf{v}_{N}^{\mathrm{T}} \right\rangle \tag{6}$$

By using Eqs. (1) to (3) and (5) in Eq. (4), the total potential energy functional can be written as

$$\Pi = \tfrac{1}{2}\mathbf{U}^{\mathrm{T}}\left(\int_L \mathbf{B}_d^{\mathrm{T}}(z)\mathbf{D}\mathbf{B}_d(z)\mathrm{d}z \right)\mathbf{U} + \tfrac{1}{2}\mathbf{U}^{\mathrm{T}}\left(\int_L \mathbf{B}_\Gamma^{\mathrm{T}}(z)\mathbf{D}_\rho\mathbf{B}_\Gamma(z)\mathrm{d}z \right)\mathbf{U} - \mathbf{F}\mathbf{U} \tag{7}$$

in which $\mathbf{B}_d(z) = \mathbf{B}'_\Gamma(z)$, $\mathbf{F}$ is the energy equivalent nodal external load vector

$$\mathbf{D} = \begin{bmatrix} E_1 A_1 & 0 & 0 \\ 0 & E_2 A_2 & 0 \\ 0 & 0 & E_1 I_1 + E_2 I_2 \end{bmatrix} \tag{8}$$

and

$$\mathbf{D}_\rho = \rho b \begin{bmatrix} 1 & -1 & -h \\ -1 & 1 & h \\ -h & h & h^2 \end{bmatrix} \tag{9}$$

where I_1 and I_2 are the second moments of area of the beams about their horizontal principal axes passing through the centroids of each cross-section. From the first variation of the total potential energy functional, the weak form of the equilibrium equations is obtained as

$$\left(\mathbf{K}_b + \mathbf{K}_s \right)\mathbf{U} = \mathbf{F} \tag{10}$$

where $\mathbf{K}_b$ is the stiffness matrix associated with the bending and the axial deformations of the beam components and $\mathbf{K}_s$ is associated with the slip energy, i.e.

$$\mathbf{K}_b = \int_L \mathbf{B}_d^{\mathrm{T}}(z)\mathbf{D}\mathbf{B}_d(z)\mathrm{d}z \tag{11}$$

and

$$\mathbf{K}_s = \int_L \mathbf{B}_\Gamma^{\mathrm{T}}(z)\mathbf{D}_\rho\mathbf{B}_\Gamma(z)\mathrm{d}z \tag{12}$$

The simplest element that satisfies the compatibility conditions can be developed by using linear interpolations for the longitudinal displacements and a cubic interpolation for the vertical displacement, i.e.

$$\mathbf{M}(z) = \left\langle \left(1 - z/L\right) \quad z/L \right\rangle \tag{13}$$

and

$$\mathbf{N}(z) = \left\langle \left(1 - \frac{3z^2}{L^2} + \frac{2z^3}{L^3} \right) \quad \left(z - \frac{2z^2}{L} + \frac{z^3}{L^2} \right) \quad \left(\frac{3z^2}{L^2} - \frac{2z^3}{L^3} \right) \quad \left(-\frac{z^2}{L} + \frac{z^3}{L^2} \right) \right\rangle \tag{14}$$

and the vector of nodal displacements **U** can be written as

$$\mathbf{U}^{\mathrm{T}} = \left\langle w_1(0) \quad w_1(L) \quad w_2(0) \quad w_2(L) \quad v(0) \quad v'(0) \quad v(L) \quad v'(L) \right\rangle \tag{15}$$

This element will be referred as the Basic Element (BE) herein. It has been reported in Dall'Asta and Zona (2004) that for stiff shear connection, BE suffers from slip-locking which is due to the fact that the discrete slip and the curvature expressions are coupled in the BE formulation, i.e., the discrete slip expression $\Gamma = <-1 \ +1 \ h> \mathbf{B}_\Gamma \mathbf{U}$ becomes

$$\Gamma = \Gamma(0)\left(1 - \frac{z}{L} \right) + \Gamma(L)\frac{z}{L} + \left(v(L) - v(0) - \frac{L}{2}[v'(L) + v'(0)] \right)\frac{6h}{L^2}\left(z - \frac{z^2}{L} \right) \tag{16}$$

where $\Gamma(0)$ and $\Gamma(L)$ are nodal slip values, i.e.

$$\Gamma(0) = w_2(0) - w_1(0) + hv'(0) \tag{17}$$

and

$$\Gamma(L) = w_2(L) - w_1(L) + hv'(L) \tag{18}$$

In the limiting case of $\rho \to \infty$ (zero slip), i.e., $\Gamma = 0$, requires the vanishing of the last term in Eq. (16) which imposes a constant value for the curvature $v'' = \mathbf{N}''(z)\mathbf{v}_N$. Locking behaviour due to this mechanism and the performance of the BE formulation are illustrated in section 4.

3.2 Finite element formulation based on the B-bar procedure

B-bar procedure (Hughes and Tezduyar 1981) provides a very easy way of modifying the basic finite element formulation since only the **B** matrices used in the stiffness matrix derivations are changed in the existing finite element analysis codes. In order to eliminate the last term in the slip expression of the basic composite beam finite element formulation in Eq. (16), the matrices $\mathbf{B}_\Gamma(z)$ and $\mathbf{B}_d(z)$ in Eqs. (11) and (12) can be directly modified as

$$\bar{\mathbf{B}}_\Gamma(z) = \begin{bmatrix} \mathbf{M}(z) & \mathbf{0} & a_1\mathbf{T}_a(z) \\ \mathbf{0} & \mathbf{M}(z) & a_2\mathbf{T}_a(z) \\ \mathbf{0} & \mathbf{0} & \mathbf{N}'(z) + a_3\mathbf{T}_b(z) \end{bmatrix} \tag{19}$$

and

$$\bar{\mathbf{B}}_d(z) = \begin{bmatrix} \mathbf{M}'(z) & \mathbf{0} & b_1\mathbf{T}_b'(z) \\ \mathbf{0} & \mathbf{M}'(z) & b_2\mathbf{T}_b'(z) \\ \mathbf{0} & \mathbf{0} & \mathbf{N}''(z) + b_3\mathbf{T}_b'(z) \end{bmatrix} \tag{20}$$

where

$$\mathbf{T}_a(z) = \left\langle 1 \quad \frac{L}{2} \quad -1 \quad \frac{L}{2} \right\rangle \tag{21}$$

and

$$\mathbf{T}_b(z) = \left\langle -1 \quad -\frac{L}{2} \quad 1 \quad -\frac{L}{2} \right\rangle \frac{z}{L}\left(1 - \frac{z}{L}\right) \tag{22}$$

and $b_1 = 3\sqrt{E_1I_1 + E_2I_2}\Big/\left(L\sqrt{2}\sqrt{E_1A_1}\right)$, $b_2 = 3\sqrt{E_1I_1 + E_2I_2}\Big/\left(L\sqrt{2}\sqrt{E_2A_2}\right)$, $b_3 = -3/L$, $a_1 = h/(2L)$, $a_2 = -6/L$. By substituting Eqs. (19) and (20) into Eq. (7), the potential energy functional becomes

$$\Pi = \tfrac{1}{2}\iint\limits_{L\ A_1} E_1\bar{\varepsilon}_1^{\,2}\mathrm{d}A\mathrm{d}z + \tfrac{1}{2}\iint\limits_{L\ A_2} E_2\bar{\varepsilon}_2^{\,2}\mathrm{d}A\mathrm{d}z + \tfrac{1}{2}\iint\limits_{L\ b} \rho\bar{\Gamma}^2\mathrm{d}x\mathrm{d}z - \Pi_{ext} \tag{23}$$

where

$$\bar{\varepsilon}_1 = \left\langle 1 \quad 0 \quad y - h_1 \right\rangle \bar{\mathbf{B}}_d \mathbf{U} \tag{24}$$

$$\bar{\varepsilon}_2 = \left\langle 0 \quad 1 \quad y - h_2 \right\rangle \bar{\mathbf{B}}_d \mathbf{U} \tag{25}$$

and

$$\bar{\Gamma} = \left\langle -1 \quad +1 \quad h \right\rangle \bar{\mathbf{B}}_\Gamma \mathbf{U} \tag{26}$$

It should be noted that, the potential energy functional in Eq. (23) should be variationally consistent in order to be used after the B-bar modifications (e.g., Simo and Hughes 1986, Prathap and Babu 1992). Variational consistency of the total potential energy functional in Eq. (23) can be verified by using the Hu-Washizu principle which is a systematic way of formulating assumed strain finite element formulations including the B-bar procedure (e.g., Simo and Hughes 1986). Thus, the Hu-Washizu functional can be written as

$$\Pi = \tfrac{1}{2}\iint\limits_{L\ A_1} E_1\bar{\varepsilon}_1^{\,2}\mathrm{d}A\mathrm{d}z + \tfrac{1}{2}\iint\limits_{L\ A_2} E_2\bar{\varepsilon}_2^{\,2}\mathrm{d}A\mathrm{d}z + \tfrac{1}{2}\iint\limits_{L\ b} \rho\bar{\Gamma}^2\mathrm{d}x\mathrm{d}z$$
$$+ \int\limits_{L}\left[\int\limits_{A_1} E_1\bar{\varepsilon}_1\left(\varepsilon_1 - \bar{\varepsilon}_1\right)\mathrm{d}A + \int\limits_{A_2} E_2\bar{\varepsilon}_2\left(\varepsilon_2 - \bar{\varepsilon}_2\right)\mathrm{d}A + \int\limits_{b} \rho\bar{\Gamma}\left(\Gamma - \bar{\Gamma}\right)\mathrm{d}x\right]\mathrm{d}z - \Pi_{ext} \tag{27}$$

in which the fourth term vanishes for the B-bar modifications introduced in Eq. (19) and (20) i.e.

$$\int\limits_{L}\left[\int\limits_{A_1} E_1\bar{\varepsilon}_1\left(\varepsilon_1 - \bar{\varepsilon}_1\right)\mathrm{d}A + \int\limits_{A_2} E_2\bar{\varepsilon}_2\left(\varepsilon_2 - \bar{\varepsilon}_2\right)\mathrm{d}A + \int\limits_{b} \rho\bar{\Gamma}\left(\Gamma - \bar{\Gamma}\right)\mathrm{d}x\right]\mathrm{d}z = 0 \tag{28}$$

where discrete strain and slip expressions are as in the Basic Element formulation, i.e., $\varepsilon_1 = \left\langle 1 \quad 0 \quad y - h_1 \right\rangle \mathbf{B}_d \mathbf{U}$, $\varepsilon_2 = \left\langle 0 \quad 1 \quad y - h_2 \right\rangle \mathbf{B}_d \mathbf{U}$ and $\Gamma = \left\langle -1 \quad 1 \quad h \right\rangle \mathbf{B}_\Gamma \mathbf{U}$. It can be verified that the potential energy functional introduced in Eq. (23) is variationally consistent. This element will

be referred to as the B-bar element BBE1. Alternatively, Eq. (28) can also be satisfied by selecting $b_1=b_2=b_3=0$ and this element will be referred herein as BBE2. The performances of BBE1 and BBE2 are illustrated in section 4.

3.3 Finite element formulation by changing the primary variables

In order to eliminate the oscillations in the slip field, the primary variables can be changed in order to consider the slip field as an independent variable so that the slip field can be directly interpolated, and the coupling between the discrete slip and the curvature can be avoided. For this purpose, the beam axis is assumed to be attached to the second component and the strain expression can be obtained by using the Euler-Bernoulli beam kinematics as

$$\varepsilon_2 = w' - yv'' \tag{29}$$

On the other hand, by considering the shift in the strain due to slip gradient as shown in Fig.1(c), the strain expression for the first component can be written as

$$\varepsilon_1 = w' - yv'' - \Gamma' \tag{30}$$

Thus, the primary variables are the longitudinal displacement of the selected axis that is attached to the second component w, the vertical displacement field v and the interlayer slip Γ. By using linear interpolation for the longitudinal displacement and slip fields, and cubic interpolation for the vertical displacement field, from Eqs. (19) and (20), the strains for both components can be written as

$$\varepsilon_1 = \langle 1 \quad -y \rangle \begin{bmatrix} \mathbf{M}'(z) & \mathbf{0} & \mathbf{M}'(z) \\ \mathbf{0} & \mathbf{N}''(z) & \mathbf{0} \end{bmatrix} \begin{Bmatrix} \mathbf{w}_N \\ \mathbf{v}_N \\ \mathbf{\Gamma}_N \end{Bmatrix} \tag{31}$$

and

$$\varepsilon_2 = \langle 1 \quad -y \rangle \begin{bmatrix} \mathbf{M}'(z) & \mathbf{0} & \mathbf{0} \\ \mathbf{0} & \mathbf{N}''(z) & \mathbf{0} \end{bmatrix} \begin{Bmatrix} \mathbf{w}_N \\ \mathbf{v}_N \\ \mathbf{\Gamma}_N \end{Bmatrix} \tag{32}$$

and the slip field can be interpolated as

$$\Gamma = \mathbf{M}(z)\mathbf{\Gamma}_N \tag{33}$$

where $\mathbf{w}_N{}^T = \langle w(0) \quad w(L) \rangle$, $\mathbf{v}_N{}^T = \langle v(0) \quad v'(0) \quad v(L) \quad v'(L) \rangle$ and $\mathbf{\Gamma}_N{}^T = \langle \Gamma(0) \quad \Gamma(L) \rangle$. By substituting Eqs. (31)-(33) into Eq. (7) and using the vector of nodal displacements based on the changed primary fields, i.e., $\mathbf{V}^T = \langle \mathbf{w}_N^T \quad \mathbf{v}_N^T \quad \mathbf{\Gamma}_N^T \rangle$, the total potential energy functional can be written as

$$\Pi = \tfrac{1}{2}\mathbf{V}^T \int_L \bar{\mathbf{B}}_1^T(z)\mathbf{D}_1\bar{\mathbf{B}}_1(z)\mathrm{d}z\,\mathbf{V} + \tfrac{1}{2}\mathbf{V}^T \int_L \bar{\mathbf{B}}_2^T(z)\mathbf{D}_2\bar{\mathbf{B}}_2(z)\mathrm{d}z\,\mathbf{V} + \tfrac{1}{2}\mathbf{V}^T \int_L \mathbf{B}_\rho^T(z)^T \rho b\mathbf{B}_\rho(z)\mathrm{d}z\,\mathbf{V} - \mathbf{F}\mathbf{V} \tag{34}$$

where

$$\mathbf{D}_1 = E_1 \begin{bmatrix} A_1 & -S_{x1} \\ -S_{x1} & I_{x1} \end{bmatrix} \tag{35}$$

$$\mathbf{D}_2 = E_2 \begin{bmatrix} A_2 & -S_{x2} \\ -S_{x2} & I_{x2} \end{bmatrix} \tag{36}$$

$$\bar{\mathbf{B}}_1(z) = \begin{bmatrix} \mathbf{N}'(z) & 0 & \mathbf{M}'(z) \\ 0 & \mathbf{M}''(z) & 0 \end{bmatrix} \tag{37}$$

$$\bar{\mathbf{B}}_2(z) = \begin{bmatrix} \mathbf{N}'(z) & 0 & 0 \\ 0 & \mathbf{M}''(z) & 0 \end{bmatrix} \tag{38}$$

and

$$\mathbf{B}_\rho(z) = \begin{bmatrix} 0 & 0 & 0 \\ 0 & 0 & 0 \\ 0 & 0 & \mathbf{M}(z) \end{bmatrix} \tag{39}$$

in which S_{x1}, I_{x1}, S_{x2} and I_{x2} are the first and second moments of area of each component of the beam with respect to the reference axis attached to the second component. From the first variation of the total potential energy functional, the weak form of the equilibrium equations can be obtained as

$$\left(\bar{\mathbf{K}}_1 + \bar{\mathbf{K}}_2 + \bar{\mathbf{K}}_\rho\right)\mathbf{V} = \mathbf{F} \tag{40}$$

where $\bar{\mathbf{K}}_1$ and $\bar{\mathbf{K}}_2$ are the stiffness matrices associated with the bending and the axial deformations of the beam components and $\bar{\mathbf{K}}_\rho$ is associated with the slip energy i.e.

$$\bar{\mathbf{K}}_1 = \int_L \bar{\mathbf{B}}_1^{\mathrm{T}}(z)\mathbf{D}_1\bar{\mathbf{B}}_1(z)\mathrm{d}z \tag{41}$$

$$\bar{\mathbf{K}}_2 = \int_L \bar{\mathbf{B}}_2^{\mathrm{T}}(z)\mathbf{D}_2\bar{\mathbf{B}}_2(z)\mathrm{d}z \tag{42}$$

and

$$\bar{\mathbf{K}}_\rho = \int_L \mathbf{B}_\rho^{\mathrm{T}}(z)^{\mathrm{T}} \rho b \mathbf{B}_\rho(z)\mathrm{d}z \tag{43}$$

In the limiting case of $\rho \to \infty$, the oscillations are eliminated in the slip field because the vanishing of the slip field ($\Gamma=0$) does not impose any constraints other than $\Gamma(L)=0$ and $\Gamma(0)=0$ as opposed to the basic finite element formulation. This element will be referred to as the Direct Slip interpolation Element (DSE) herein. The performance of DSE is illustrated in the following section.

4. Applications

The performances of the developed elements DSE, BBE1 and BBE2 are illustrated in this section. In all cases the total span of the beam is taken as $L=10$ m. The top component of the cross-section has a modulus of elasticity of $E_1=26\times10^3$ MPa. The width and the thickness of the rectangular top section (Fig. 1(a)) are $B_d=600$ mm and $t_d=15$mm, respectively. The modulus of elasticity of the bottom component is $E_2=200\times10^3$ MPa. The overall height, flange width, flange thickness and web thickness of the bottom I-section are $D_g=412$ mm, $B_g=200$ mm, $t_f=12$ mm and $t_w=8$ mm, respectively. The beam axis is selected at the centroid of the bottom component. Analyses were undertaken for two different connection stiffness parameters $\rho=0.1$ N/mm^3 ($\alpha L=2.973$) and $\rho=100$ N/mm^3 ($\alpha L=94.016$). The effective intersection surface width between the two components is taken as $b=150$ mm based on which the dimensionless connection stiffness parameter can be calculated as (Dall'Asta and Zona 2004)

$$\alpha = \sqrt{\rho b\left(\frac{1}{E_1A_1}+\frac{1}{E_2A_2}+\frac{h^2}{E_1I_1+E_2I_2}\right)} \tag{44}$$

The results are compared with those based on the discrete strain gap method developed in (Erkmen and Bradford 2011a) and denoted herein as DE which can also be considered as a special case of the B-bar procedure in which $\bar{\mathbf{B}}_\Gamma$ matrix in Eq. (19) was replaced with

$$\bar{\mathbf{B}}_\Gamma = \begin{bmatrix} \dfrac{1}{2} & \dfrac{1}{2} & 0 & 0 & 0 & 0 & 0 & 0 \\ 0 & 0 & \dfrac{1}{2} & \dfrac{1}{2} & 0 & 0 & 0 & 0 \\ 0 & 0 & 0 & 0 & \dfrac{-1}{L} & 0 & \dfrac{1}{L} & 0 \end{bmatrix} \tag{45}$$

and $b_1=b_2=b_3=0$ were used in Eq. (20). The exact solutions are also obtained based on the finite element procedure developed in (Erkmen and Bradford 2011a) and denoted herein as EE which provides benchmark data for comparison purposes. It should also be noted that the element BBE2 developed herein is identical with AE given in (Erkmen and Bradford 2011a). However, by directly replacing $\bar{\mathbf{B}}_\Gamma$ with $\mathbf{B}_\Gamma$ the static condensation step can be prevented.

4.1 Simply supported beam

For the simply supported case (i.e., $v(0)=w_2(0)=v(L)=0$) the beam is subjected to a 5kN vertical mid-span load. Analyses were made for one-, two- and four-element models. Fig. 2 shows the vertical deflections at the centroid of the bottom component, the interlayer slip, and the curvatures based on four-element solutions. The convergence rates (i.e., p in $||e||_{en}=Ch^p$ where C is an arbitrary constant and h is the element size) of the elements are shown in log-log scale in Figs. 3 (a) and (b). The effect of the shear connection stiffness on the error in the total strain energy is shown in Fig. 4. From Fig. 2 (a), it can be verified that for the flexible shear connection ($\rho=0.1$ N/mm^3) deflections based on the BE, BBE2, DSE and DE are close to the exact solution EE. Only,

(a) Vertical displacement (ρ=0.1 N/mm^3) (b) Vertical displacement (ρ=100 N/mm^3)

(c) Slip (ρ=0.1 N/mm^3) (d) Slip (ρ=100 N/mm^3)

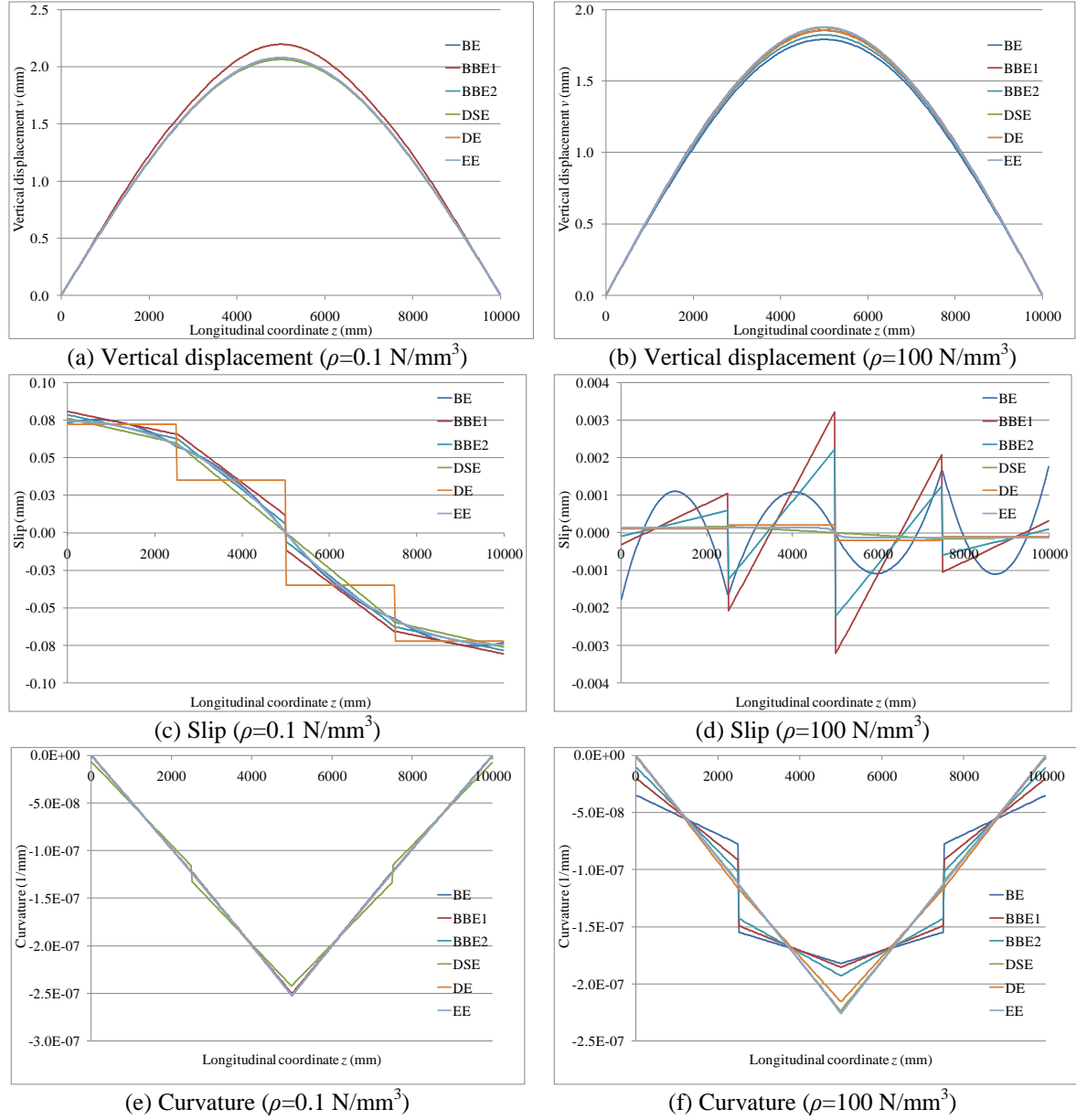(e) Curvature (ρ=0.1 N/mm^3) (f) Curvature (ρ=100 N/mm^3)

Fig. 2 Analysis results for the simply supported beam

BBE1 depicts a softer behaviour than the exact solution. The mid-span values based on BE, BBE1, BBE2, DSE, DE and EE are 2.075 mm, 2.197 mm, 2.075 mm, 2.064 mm, 2.080 mm and 2.079 mm, respectively. On the other hand as shown in Fig. 2(b), for the stiff shear connection (ρ=100 N/mm^3) BE depicts a stiffer behaviour than the exact solution EE due to locking effects. The mid-span values for the stiff connection case based on BE, BBE1, BBE2, DSE, DE and EE reduce to 1.791 mm, 1.873 mm, 1.856 mm, 1.823 mm, 1.854 mm and 1.878 mm, respectively. The effects of locking can also be observed from the slip results. In Fig. 2(c), quadratic slip results based on BE

(a) Convergence rate (ρ=0.1 N/mm^3)

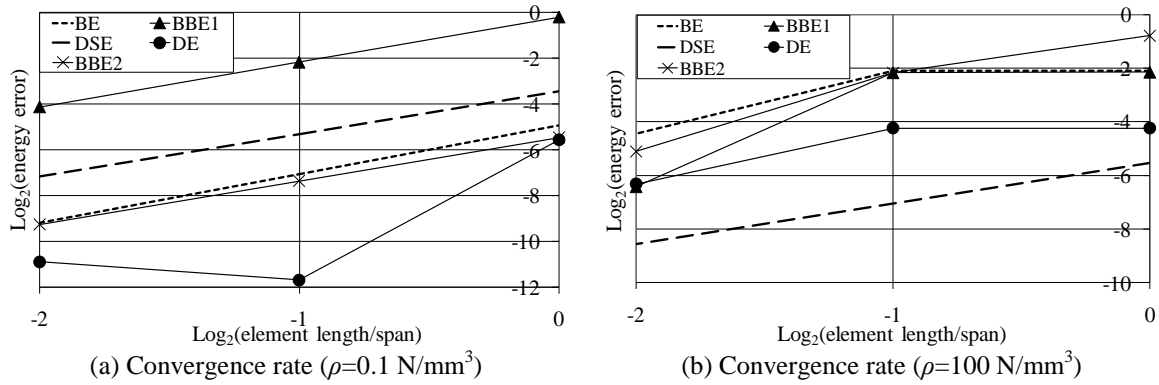(b) Convergence rate (ρ=100 N/mm^3)

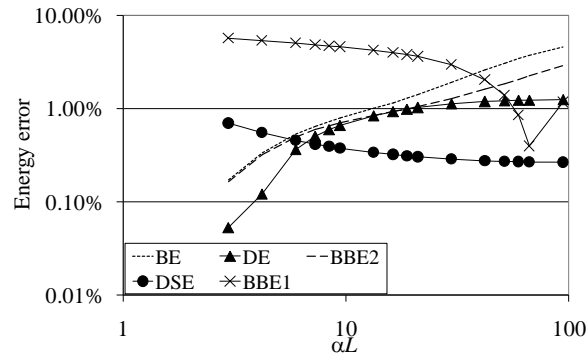Fig. 3 Accuracy and convergence rate for the simply supported beam

Fig. 4 Energy error versus connection stiffness based on four elements

as well as linear slip results based on elements BBE1, BBE2, DSE and mid-values of the constant slip based on element DE are accurate for the flexible shear connection case. The effects of locking can be observed from the oscillations in the slip results of BE, BBE1 and BBE2 for the stiff shear connection case (ρ=100 N/mm^3) in Fig. 2(d). On the other hand, results of DE and DSE are very accurate as they follow the exact curve. It should be noted that the results of the B-bar elements BBE1, BBE2 and DE always intersect at a point that is very close to the exact solution as can be verified from Fig. 2(d) which suggests the existence of a superconvergent point for the B-bar procedure. Locking effects can also be observed from the comparison of the curvature results in Figs. 2 (e) and (f) as the curvature based on elements BE, BBE1, BBE2 tend to become constant within an element which causes the inter-element dislocation. On the other hand, curvature results based on DE and DSE are accurate in both stiff and flexible connection cases while results of DSE are the most accurate and very close to the exact solution.

From Figs. 3 (a) and (b) it can be verified that the average slopes for the flexible connection case for elements BE, BBE1, BBE2 and DE are 2.12, 1.96, 1.89 and 2.66 respectively. These slopes change to 1.18, 2.13, 2.16 and 1.03, respectively for the stiff connection case. The convergence rate of element DSE is only slightly affected by the connection stiffness since the average slope of the curve 1.86 for the flexible connection case reduces slightly to 1.51 for the stiff connection case. However, the accuracy of the element DSE improves slightly for the stiff connection case.

(a) Vertical displacement ($\rho=0.1$ N/mm^3)

(b) Vertical displacement ($\rho=100$ N/mm^3)

(c) Slip ($\rho=0.1$ N/mm^3)

(d) Slip ($\rho=100$ N/mm^3)

(e) Curvature ($\rho=0.1$ N/mm^3)
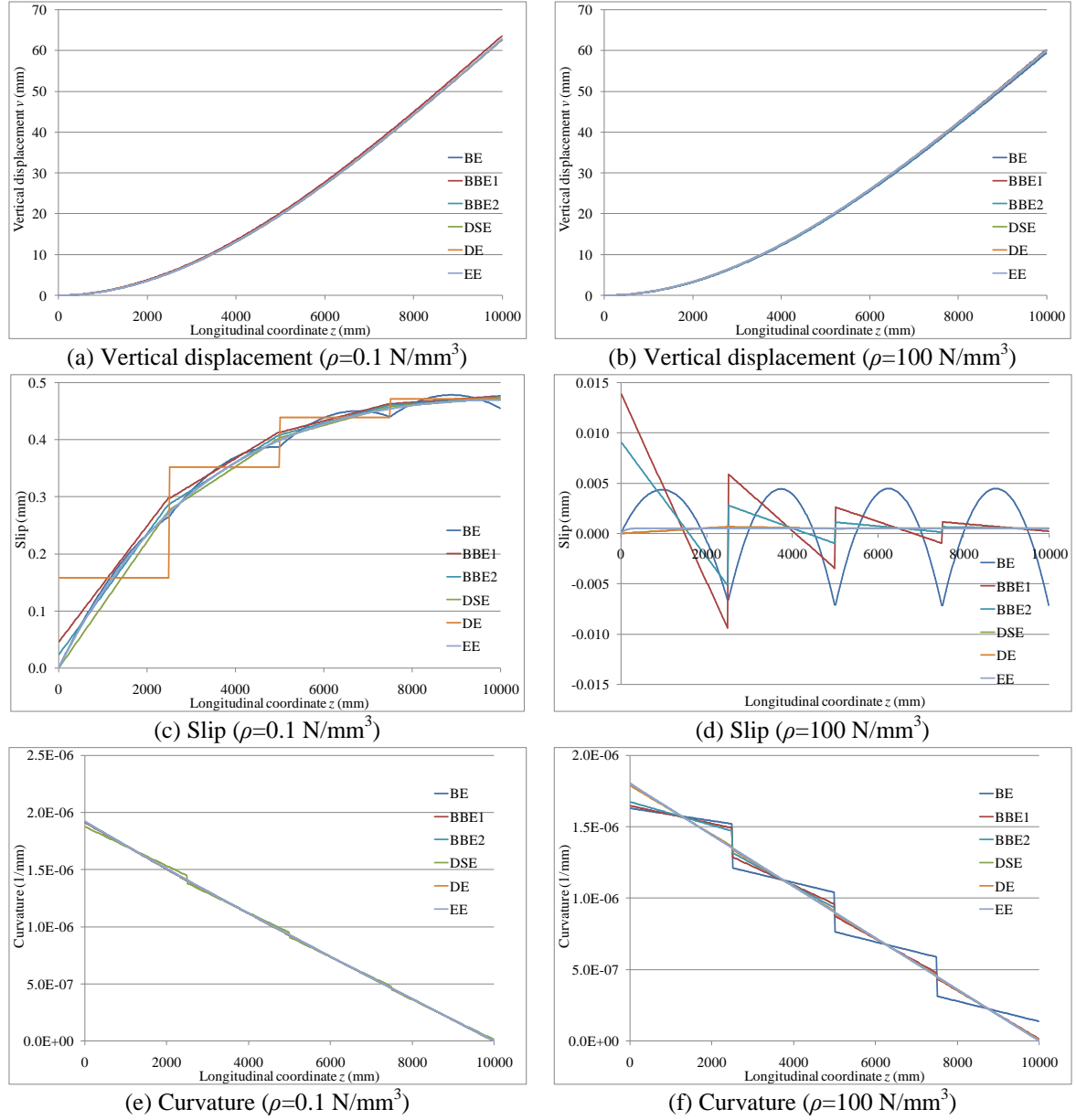
(f) Curvature ($\rho=100$ N/mm^3)

Fig. 5 Analysis results for the cantilever beam

The favourable effect of the connection stiffness on the behaviour of element DSE can be verified from Fig. 4 as it shows that the energy error reduces when the connection stiffness is increased which also has the greatest accuracy for $\alpha L=94.016$. It can also be observed from Fig. 4 that the error in elements BE, BBE2 and DE increases for stiffer connections. The developed element DSE shows an excellent performance since in the stiff connection case the oscillations are prevented and the energy error is not affected adversely. The B-bar element BBE2 also has a superior performance to BE.
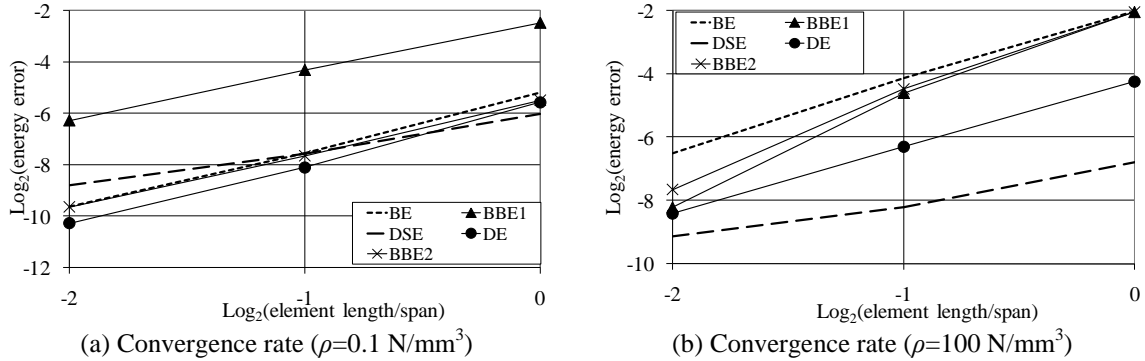
(a) Convergence rate (ρ=0.1 N/mm^3) (b) Convergence rate (ρ=100 N/mm^3)

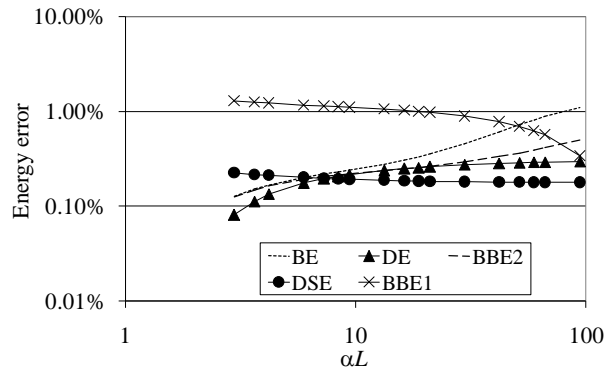Fig. 6 Accuracy and convergence rate for the cantilever beam

Fig. 7 Energy error versus connection stiffness based on four elements

4.2 Cantilever beam

The second example is that of a cantilever beam-column (i.e., $v(0)=v'(0)=w_1(0)=w_2(0)=0$) subjected to a 10kN vertical load acting at the tip. Finite element analyses were made for one-, two- and four-element models. Fig. 5 shows the vertical deflection, longitudinal slip and the curvatures based on the four-element finite element model. The convergence and accuracy performances of the elements with different connection stiffnesses based on the energy norm are given in Fig. 6. The effect of the shear connection stiffness on the error in the total strain energy is shown in Fig. 7. Similarly to the simply supported case, all elements provide sufficiently accurate results for the flexible connection; however for stiff shear connection element BE shows severe oscillations in the slip values, and the accuracy of the results diminish. Fig. 5(d) shows that the slip results for elements BBE1 and BBE2 also oscillate for the stiff connection; however the intersection-point values are accurate.

The average slopes for the flexible connection case for elements BE, BBE1, BBE2, DE and DSE are 2.21, 1.90, 2.08, 2.35 and 1.39, respectively which change to 2.24, 3.08, 2.80, 2.08 and 1.17 respectively for the stiff connection case; as shown in Figs. 6 (a) and (b).

Fig. 7 shows that formulation DSE is not affected by the connection stiffness while the error in elements BE, BBE2 and DE are only slightly increased for stiffer connections. The developed element DSE again depicts excellent behaviour for the cantilever beam case.
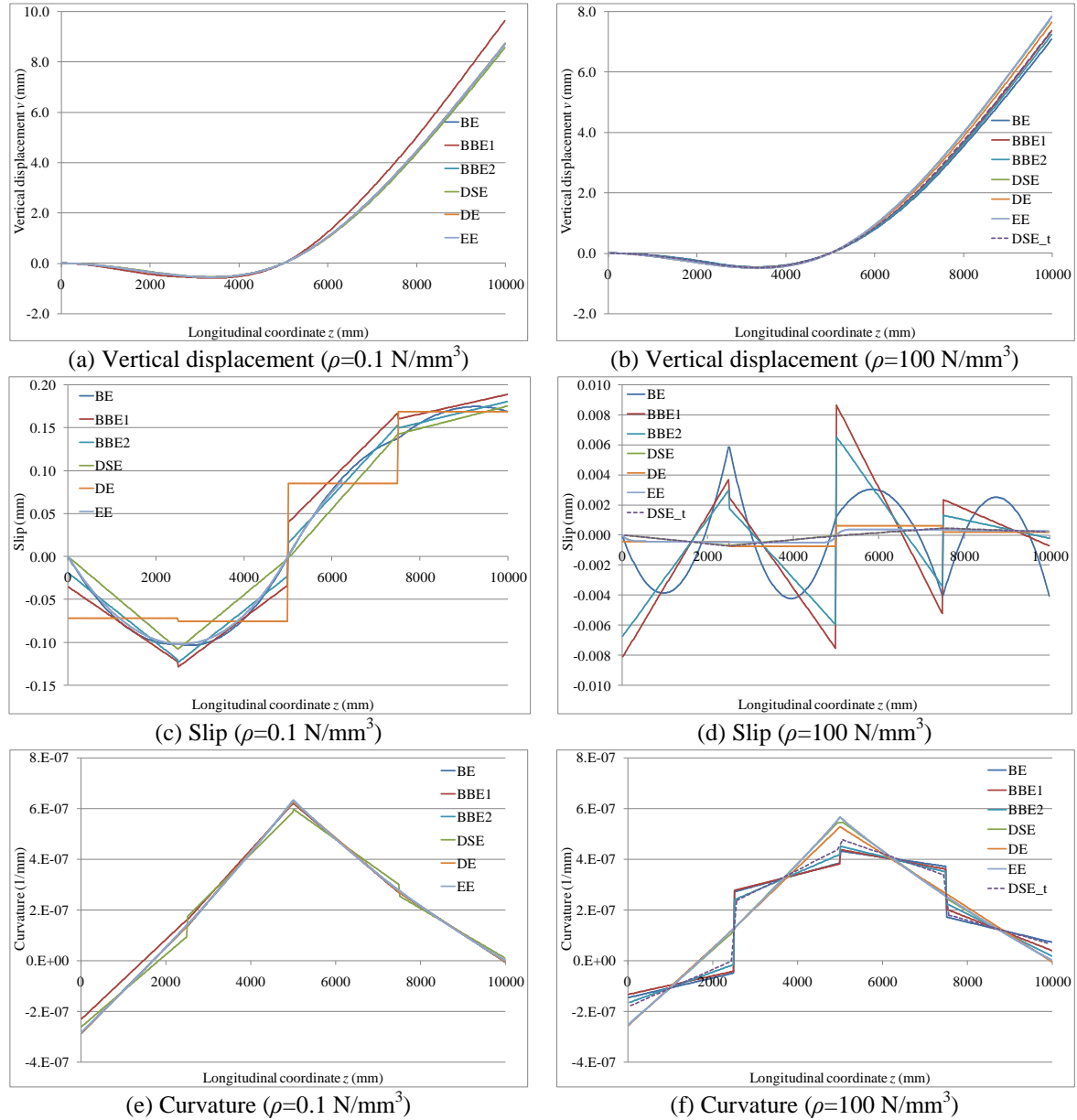
(a) Vertical displacement (ρ=0.1 N/mm^3)

(b) Vertical displacement (ρ=100 N/mm^3)

(c) Slip (ρ=0.1 N/mm^3)

(d) Slip (ρ=100 N/mm^3)

(e) Curvature (ρ=0.1 N/mm^3)

(f) Curvature (ρ=100 N/mm^3)

Fig. 8 Analysis results for the propped cantilever

4.3 Propped cantilever beam

The last example is that of a cantilever beam which is propped at its mid-span (i.e., $v(0)=v'(0)=w_1(0)=w_2(0)=v(L/2)=0$) and subjected to a 0.5kN/m vertical uniformly distributed load and 5kN vertical point load at the free end. Finite element analyses were made for two-, four- and eight-element models. The deflections and curvatures are shown in Fig. 8. Fig. 9 shows the convergence and accuracy performance of each element based on flexible and stiff connection

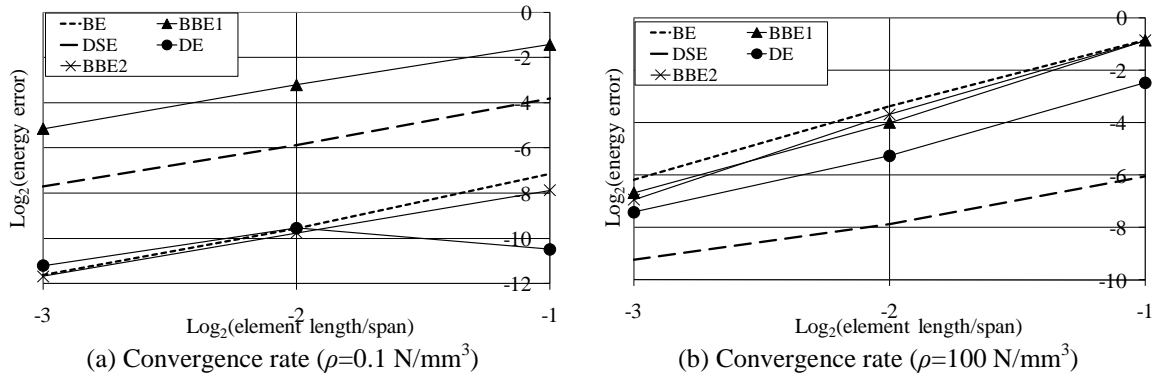(a) Convergence rate (ρ=0.1 N/mm^3) (b) Convergence rate (ρ=100 N/mm^3)

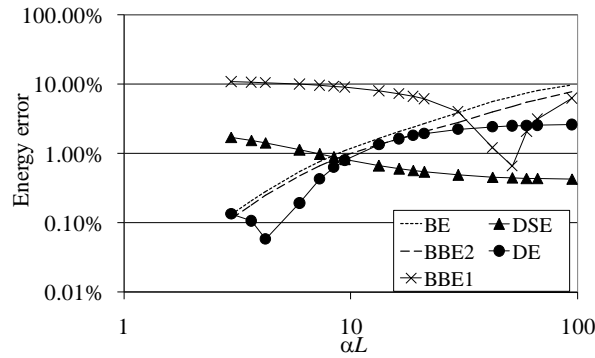Fig. 9 Accuracy and convergence rate for the propped cantilever

Fig. 10 Energy error versus connection stiffness based on four elements

cases. Fig. 10 shows the dependence of the energy error on the connection stiffness. From Fig. 8(a), it can be verified that for the flexible shear connection deflections based on the BE, BBE2, DSE and DE are close to the exact solution EE. Only, BBE1 depicts a softer behaviour than the exact solution similar to the simply supported case. The tip values based on BE, BBE1, BBE2, DSE, DE and EE are 8.706 mm, 9.637 mm, 8.707 mm, 8.572 mm, 8.729 mm and 8.737 mm, respectively. On the other hand as shown in Fig. 8(b), the tip deflection values change to 7.092 mm, 7.366 mm, 7.246 mm, 7.707 mm, 7.645 mm and 7.859 mm, respectively for the stiff connection case. Fig. 8(d) shows that oscillations that occur in stiff connection due to locking in element BE are circumvented when elements DE and DSE are used. Also, the slip values at the intersection points of elements BBE1, BBE2 are very close to the exact results.

The average slopes for the convergence rates for the flexible connection case for elements BE, BBE1, BBE2, DE and DSE are 2.23, 1.86, 1.90, 0.36 and 1.95, respectively which change to 2.68, 2.91, 3.05, 2.47 and 1.59, respectively for the stiff connection case as shown in Figs. 9 (a) and (b).

Fig. 10 shows that element DSE is not affected by the connection stiffness and therefore shows excellent performance.

4.4 Curvature-locking with direct slip interpolation element

In the conventional finite element formulation BE curvature-locking is associated with slip-

locking as a stiff connection imposes a constant value on curvature as discussed herein. When element DSE is used, slip-locking is completely eliminated for stiff connections. However, the curvature can still have the tendency to become constant within the element, and thus DSE is prone to curvature-locking (without accompanying oscillations in the slip field). For instance, when the average strain at the centroid of the second (bottom) component approaches zero due to the fact that the second component is significantly more rigid than the first (top) component and the shear connection is stiff, i.e., $\Gamma' \to 0$, the strain at the centroid of the second component can be expressed by using Eq. (29) as

$$w' - h_2 v'' \to 0 \tag{46}$$

Since linear interpolation is used for axial deflection w, Eq. (46) constrains the curvature to be a constant term. Curvature-locking in the case of a rigid second component can be avoided however, by selecting the arbitrary axis to pass through the centroid of the second component, i.e., $h_2 = 0$ and vice versa. Similarly, when one of the components is significantly rigid in comparison to the other, it does not cause curvature-locking when elements BE, DE, BBE1 or BBE2 are used, since Eq. (1) and/or Eq. (2) is used to express the strains at the centroids of the components and thus, the strains at the centroids are not affected by the curvature. The curvature-locking behaviour with element DSE is created by shifting the axis to the centroid of the top component instead of the bottom component as used in the previous cases since the top component is the softer component. In this case, the results based on the element DSE are shown as DSE_t in Figs. 8 (b), (d) and (f). From Fig. 8 (d) it can be verified that the slip behaviour of DSE_t matches with that of DSE, hence slip-locking does not occur; however the inter-element curvature jumps become significant as the curvature tends to become constant in each element as shown in Fig. 8(f). Curvature-locking in the case of the analysis with DSE_t also causes stiffer behaviour for the beam in comparison to the analysis with DSE, as can be observed from Fig. 8(b).

5. Conclusions

The displacement-based finite element formulation founded on a linear interpolation of the longitudinal displacement fields and the cubic interpolation of the vertical displacement field suffers from locking when used for the analysis of composite beam-columns consisting of two Euler-Bernoulli beams juxtaposed with a deformable shear connection. The main problem with the conventional displacement-based formulation is that for stiff connections the nodal values of slip may be totally erroneous and severe oscillations occur in the slip field. In this study, the displacement based finite element formulation was modified by using the B-bar procedure which is a very easy way of modifying the basic finite element formulations since only the **B** matrices used in the stiffness matrix derivations are changed in the existing finite element analysis code. Examples have shown that slip values based on B-bar elements coincide at a point. These intersection points provide very accurate slip results at the element level which suggests the existence of a super-convergent point for the B-bar procedure. By changing the primary variables, to be able to interpolate the slip field directly, an efficient finite element was also developed which completely eliminates the oscillatory slip behaviour and degradations in the accuracy for stiff shear connections. It was shown that the element developed by changing the primary variables may still suffer from curvature-locking, however by proper selection of the beam axis curvature locking can be alleviated.

References

Arizumi, Y., Yamada, S. and Kajita, T. (1981), "Elastic-plastic analysis of composite beams with incomplete interaction by finite element method", *Comput. Struct.*, **14**, 543-462.

Ayoub, A. and Filippou, F.C. (2000), "Mixed formulation of nonlinear steel-concrete composite beam elements", *J. Struct. Eng.*, ASCE, **126**(3), 371-381.

Ayoub, A. (2005), "A force-based model for composite steel-concrete beams with partial interaction", *J. Const. Steel Res.*, **61**, 387-414.

Cho, J.Y. and Atluri, S.N. (2001), "Analysis of shear flexible beams, using the meshless local Petrov-Galerkin method, based on a locking-free formulation", *Eng. Comput.*, **18**, 215-240.

Dall'Asta, A. and Zona, A. (2002), "Non-linear analysis of composite beams by a displacement approach", *Comput. Strutct.*, **80**, 2217-2228.

Dall'Asta, A. and Zona, A. (2004a), "Three-field mixed formulation for non-linear analysis of composite beams with deformable shear connection", *Finite Elem. Anal. Des.*, **40**(4), 425-448.

Dall'Asta, A, and Zona, A. (2004b), "Slip locking in finite elements for composite beams with deformable shear connection", *Finite Elem. Anal. Des.*, **40**, 1907-1930.

Daniels, B. and Crisinel, M. (1993), "Composite slab behaviour and strength analysis. Part I: Calculation procedure", *J. Strutc. Eng.*, ASCE, **119**(1), 16-35.

Erkmen, R.E. and Bradford, M.A. (2009), "Non-linear elastic analysis of composite beams curved in-plan", *Eng. Struct.*, **31**(7), 1613-1624.

Erkmen, R.E. and Bradford, M.A. (2010a), "Locking-free finite element formulation for steel concrete composite members", *Proceedings of the 9th World Congress on Comput. Mech.,* Sydney, Australia.

Erkmen, R.E. and Bradford, M.A. (2010b), "Elimination of slip-locking in composite beam-column analysis by using the element-free Galerkin method", *Comput. Mech.*, **46**, 911-924.

Erkmen, R.E. and Bradford M.A. (2011a), "Treatment of slip-locking for displacement based finite element analysis of composite beam-columns", *Int. J. Numer. Meth. Eng.*, **85**(11), 805-826.

Erkmen, R.E. and Bradford, M.A. (2011b), "Time-dependent creep and shrinkage analysis of composite beams curved in-plan", *Comput. Struct.*, **89**, 67-77.

Faella, C., Martinelli, E. and Nigro, E. (2002), "Steel and concrete composite beams with flexible shear connection: exact analytical expression of the stiffness matrix and applications", *Comput. Struct.*, **80**, 1001-1009.

Hughes, T.J.R. and Tezduyar, T.E. (1981), "Finite elements based upon Mindlin Plate theory with particular reference to the four node bilinear isoparametric element", *J. Appl. Mech.*, ASME, **48**(3), 587-596.

Newmark, N.M., Siess, C.P. and Viest, I.M. (1951), "Tests and analysis of composite beams with incomplete interaction", *Proc. Soc. Exp. Struct. Anal.*, **9**(1), 75-92.

Martinelli, E., Nguyen, Q.H. and Hjiaj, M. (2012), "Dimensionless formulation and comparative study of analytical models for composite beams in partial interaction", *J. Const. Steel Res.*, **75**, 21-31.

Nguyen, Q-H., Hjiaj, M. and Guezouli, S. (2011), "Exact finite element model for shear-deformable two-layer beams with discrete shear connection", *Finite Elem. Anal. Des.,* **47**, 718-727.

Nguyen, Q-H., Martinelli, E. and Hjiaj, M. (2011), "Derivation of the exact stiffness matrix for a two-layer Timoshenko beam element with partial interaction", *Eng. Struct.,* **33**, 298-307.

Prathap, G. and Babu, C.R. (1992), "Stress oscillations and spurious load mechanism in variationally inconsistent assumed strain formulations", *Int. J. Num. Meth. Eng.*, **33**, 2181–2197.

Pi, Y.L., Bradford, M.A. and Uy, B. (2006), "Second order nonlinear inelastic analysis of composite steel-concrete members. I: Theory", *J. Struct. Eng.*, **132**(5), 751-761.

Ranzi, G. and Bradford M.A. (2009), "Analysis of composite beams with partial interaction using the direct stiffness approach accounting for time effects", *Int. J. Numer. Meth. Eng.*, **78**(5), 564-586.

Ranzi, G., Bradford, M.A. and Uy, B. (2004), "A direct stiffness analysis of a composite beam with partial interaction", *Int. J. Num. Meth. Engrg.*; Vol. **61**, 657-672.

Salari, M.R., Spacone, E., Shing, P.B. and Frangopol, D.M. (1998), "Nonlinear analysis of composite beams

with deformable shear connectors", *J. Struct. Eng.*, ASCE, **124**(10), 1148-1158.

Simo, J.C. and Hughes, T.J.R. (1986), "On the variational foundations of assumed strain methods ", *J. Appl. Mech.*, ASME, **53**, 51-54.